Electronic Supplementary Material (ESI) for Journal of Materials Chemistry C.

Supporting Information

Organic Microcrystal Array-Embedded Layer: Highly Directional Alternating *p*- and *n*-Channel for Ambipolar Transistor and Inverter

Minkyung Jea, Amit Kumar, Hyejin Cho, Dongmyung Yang, Hyunseok Shim, Akshaya K. Palai, Seungmoon Pyo*

Department of Chemistry, Konkuk University, 120 Neungdong-ro, Gwangjin-gu, Seoul 143-701, Republic of Korea

Corresponding author: pyosm@konkuk.ac.kr

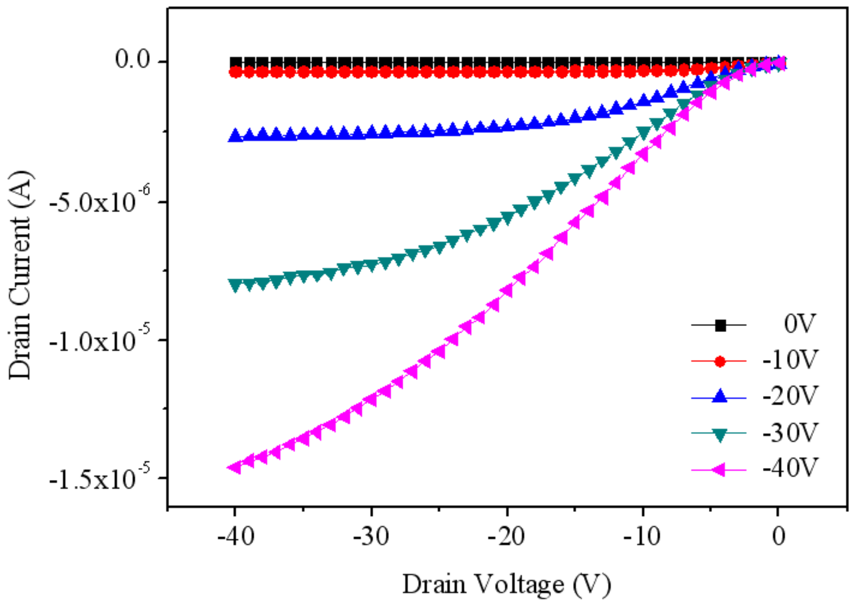

Fig. S1 Output (V_{GS} = 0 V ~ -40 V) characteristic curves of OFETs based on TIPS-pentacene 1D-microwires and 480 nm thick polymer gate dielectric. The channel length (L) and width (W) of the OFET were 50 and 64 μm, respectively.

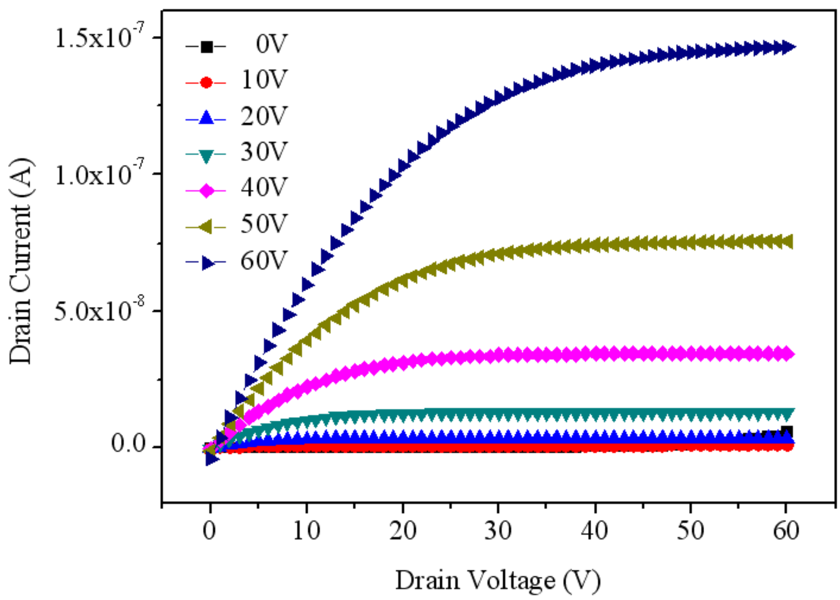

Fig. S2 Output (V_{GS} = 0 V ~ 60 V) characteristic curves of OFETs based on a single layer of $F_{16}CuPc$ (50 nm) thin-film grown by thermal evaporation on CL-PVP gate dielectric at room temperature. The channel length (L) and width (W) of the OFETs were 50 and 1000 μm, respectively.

Morphological characteristics of $F_{16}CuPc$ film deposited on and in between the TIPS-pentacene microwires.

AFM images of the $F_{16}CuPc$ film deposited on and in between 1D-microwires of TIPS-pentacene are shown in Fig. S3. This figure shows the topology of $F_{16}CuPc$ deposited on 1D-microwires of TIPS-pentacene [Fig. S3(a)] and in between the microwires [Fig. S3(b)]. Figures also show that the grain sizes of the deposited $F_{16}CuPc$ on 1D-microwires are smaller in comparison to the grain sizes deposited in between 1D-microwires. The average and rms roughness of $F_{16}CuPc$ film deposited on 1D-microwires are 0.875 and 1.105 nm, respectively. The average and rms roughness of $F_{16}CuPc$ film deposited in between the 1D-microwires are 0.921 and 1.161 nm, respectively.

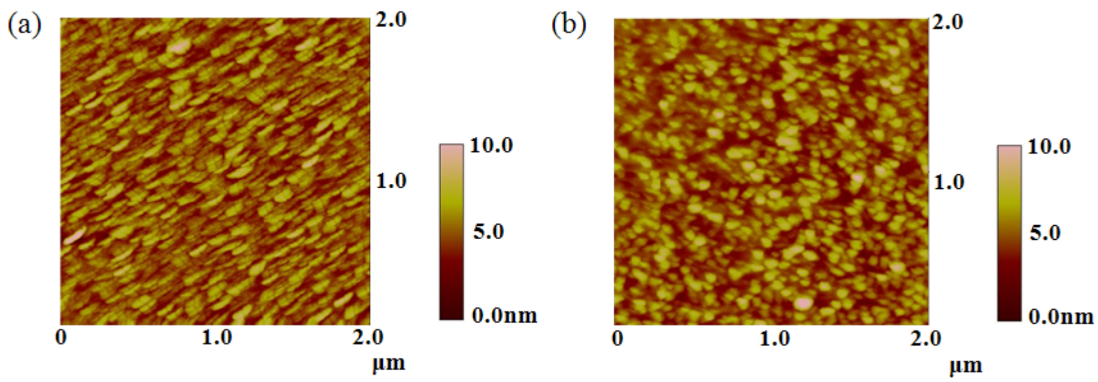

Fig. S3 (a) AFM images (2 x 2 μm^2).of $F_{16}CuPc$ film grown on 1D-microwires of TIPS-pentacene at 25 ^oC; (b) AFM images of $F_{16}CuPc$ film grown on polymer gate dielectric (in between the microwires) at 25 ^oC.

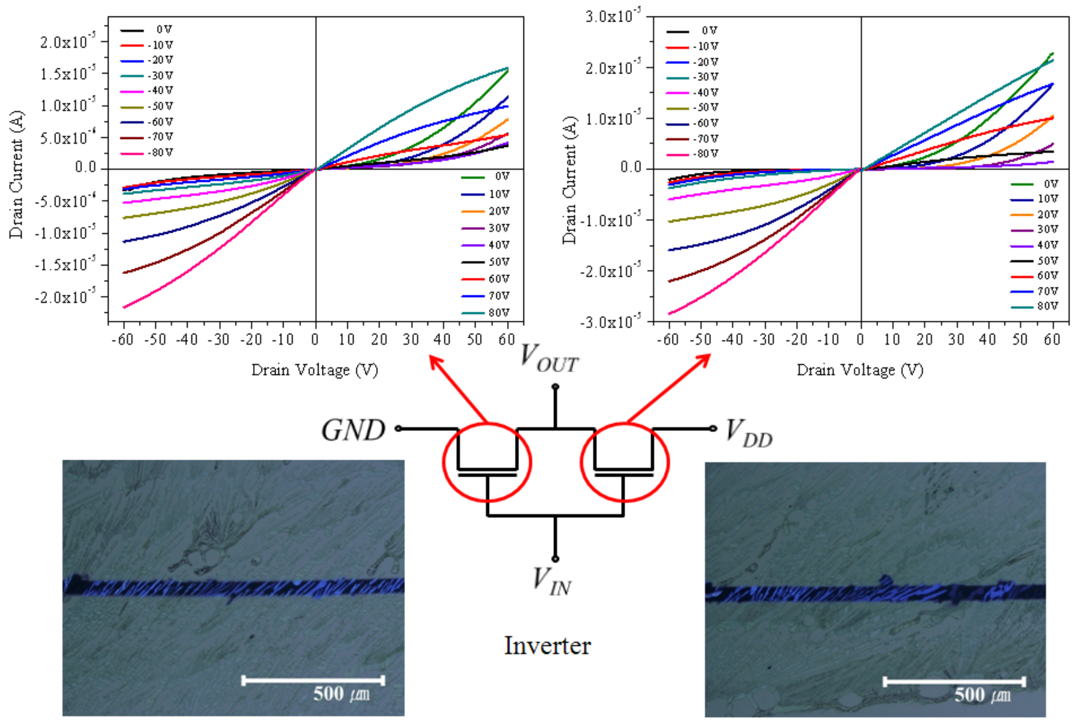

Fig. S4 Output curves of the CMOS-like inverter based on two ambi-OFETs based on alternating *p*- and *n*-channel along with the schematic diagram of the logic circuit and optical microscopic image of the channel region of both OFETs. Output characteristics of ambi-OFETs swept from V_{DS} 0 V to 60 V with an increment of 1 V with an applied constant V_{GS} from 0 V to 80 V (increment of 10 V). Similarly, output characteristics of ambi-OFETs were measured by sweeping from V_{DS} 0 V to -60 V (increment of 1 V) with an applied constant V_{GS} from 0 V to -80 V (increment of -10 V).

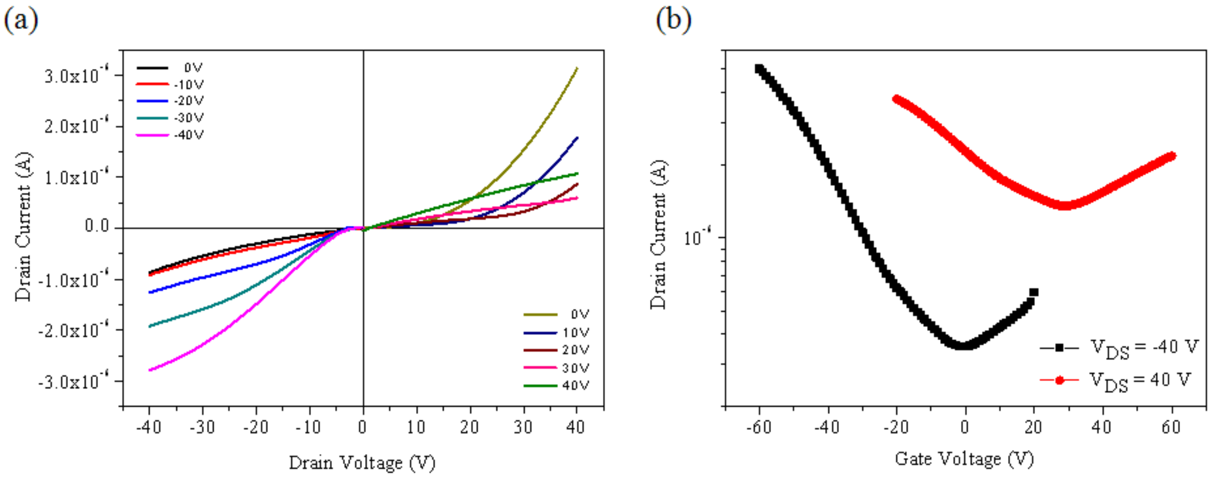

Fig. S5 (a) Output and (b) transfer characteristics of the ambi-OFET used in load type inverter.

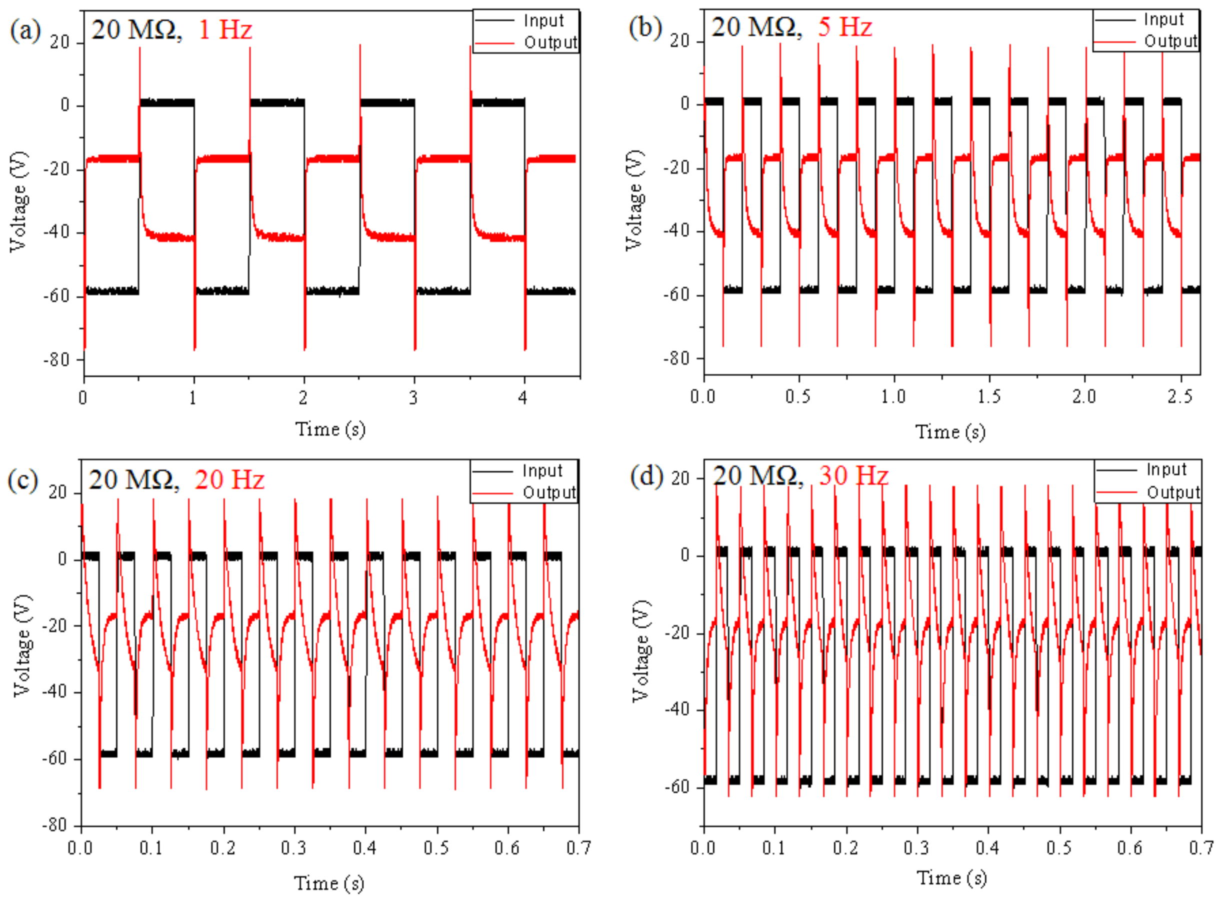

Fig. S6 The transient response of PMOS with a resistive load of 20 MΩ at constant drain bias when the gate voltage is pulsed at (a) 1 Hz, (b) 5 Hz, (c) 20 Hz and (d) 30 Hz.

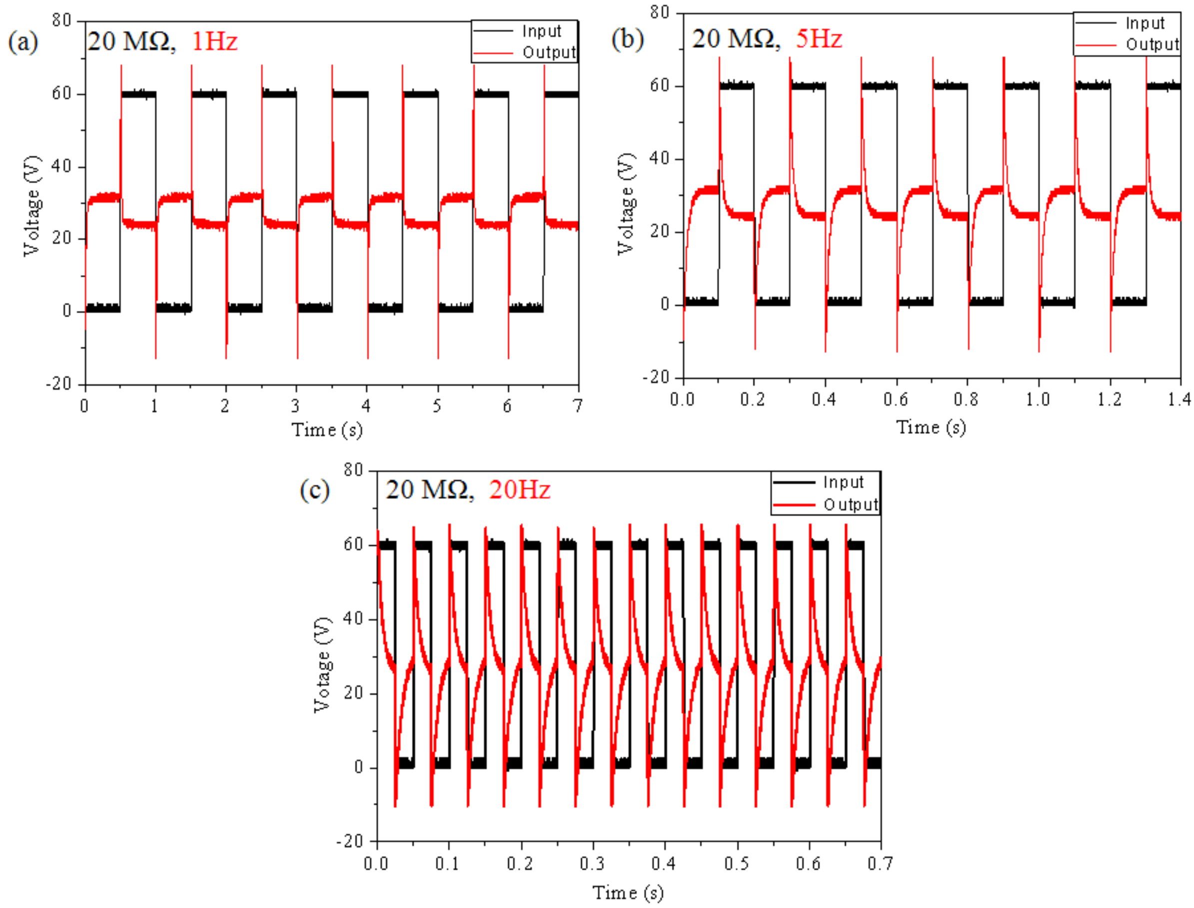

Fig. S7 The transient response of NMOS with a resistive load of 20 MΩ at constant drain bias when the gate voltage is pulsed at (a) 1 Hz, (b) 5 Hz, and (c) 20 Hz.